CHAPTER VIII

FORMATION MECHANISMS OF CARBON MICROSPHERES

8.1 Introduction

The visual appearance of the CMSs obtained from the glucose experiment was similar to that from the other carbohydrates. In fact, the CMSs have a dark brown color for the glucose experiment but the CMSs from others (native corn starch, amylose, amylopectin, and HI-CAP®100) have a black color. The CMS particles were precipitated in bottom of reactor. The CMSs particles from glucose have a small size than those from other carbohydrates. The FT-IR spectroscopy of the CMS particles obtained from glucose were carried out and compared with those obtained from other carbohydrate experiment. Moreover, in order to insight gain more information about carbon microsphere (CMSs), the CMS particles from different precursors (glucose or native corn starch) was determined their compositions by elemental analysis. In addition, internal structure of CMSs was provided by transmission electron microscopy in order to reveal their core/shell structure.

8.2 Characterization procedures

The CMS particles in all experiments are water-insoluble product. Only a portion of the solid particles dissolve in organic solvents such as acetone, methanol, hexane, or tetrahydrofuran [71]. Functional group and chemical structure were characterized by Fourier Transform Infrared Spectroscopy (PerkinElmer). Elemental analysis of CMSs was analyzed by CHNS/O analyzer (Perkin Elmer PE2400 Series II). Gaseous products freed by pyrolysis in high-purity oxygen and were chromatographically separated by frontal analysis with quantitatively detected by thermal conductivity detector. Core/shell structure of CMSs was revealed by transmission electron microscopy (JEOL, JEM-2100).

8.3 Results and discussion

8.3.1 Carbon microspheres compositions

As described in previous chapter, yield (based on carbon yield) of synthesized CMSs was depended on reaction time and temperature. When CMS formation completed, the highest yield obtained about 80%. Elemental compositions of carbon microspheres were analyzed by CHNS/O analyzer (Perkin Elmer PE2400 Series II). In this analysis, gaseous products freed by pyrolysis in high-purity oxygen and were chromatographically separated by frontal analysis with quantitatively detected by thermal conductivity detector. In this analysis, nitrogen and sulfur in products were neglected because of small quantity. The elemental chemical compositions (C, O, and H) of pure glucose, starch, and different CMS samples are listed in Table 8.1. It can be seen that the carbon content increases from 40% in the glucose to approximately 60% (sample: GC, 10wt%, 180°C, 24h) in the CMS samples. At the same time there is a reduction in the oxygen and hydrogen contents. These variations become greater as the reaction temperature increases, which is consistent with a carbonization process.

Table 8.1 Chemical compositions of glucose, starch and as-prepared CMSs

Samples	C[wt%]	H[wt%]	O[wt%]	O/C[a]	H/C[a]
Glucose	40.00	6.67	53.33	1.00	2.00
Starch (CR, AP, AL, HI-CAP®100)	44.44	6.17	49.38	0.83	1.67
GC 10wt% 180°C 24h	60.00	4.81	35.04	0.44	0.69
HICAP 10wt% 180°C 24h	65.02	4.54	30.21	0.35	0.84
AP 10wt% 180°C 24h	63.65	4.42	31.68	0.37	0.83
AL 10wt% 180°C 24h	65.72	4.67	29.21	0.33	0.85
AP+AL 10wt% 180°C 24 h	63.89	4.42	31.34	0.37	0.83
CR 10wt% 180°C C 24h	67.63	4.49	27.50	0.30	0.80
CR 10wt% 180°C 18h	65.65	4.50	29.55	0.34	0.82
CR 10wt% 180°C 6h	63.88	4.70	31.01	0.36	0.88
CR 10wt% 220°C 6h	68.89	4.59	26.27	0.29	0.80

Note: [a] = atomic ratio, CR = native corn starch, AP = amylopectin, AL = amylose

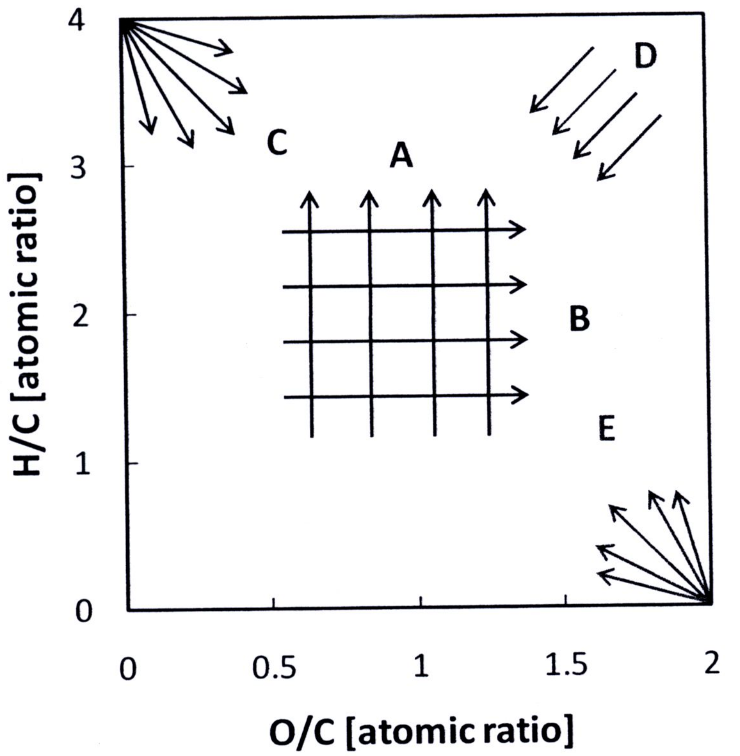

Figure 8.1 van Krevelen diagram for prediction of reactions: A=hydrogenation reaction, B=Oxidation reaction, C = demethanation reaction, D = dehydration reaction and E = decarboxylation reaction [72]

In chemical transformation, van Krevelen diagram was used to determine overall reaction which occurred in the chemical transformations [72]. Van Krevelen calculated some trajectories appropriate to this type of plot for general chemical reactions such as hydrogenation, oxidation, dehydration etc., as shown in Figure 8.1. Increases in the O/C ratio at constant H/C ratio, i.e. straight lines parallel to the O/C axis, (**B** in Figure 8.1), are obviously oxidation paths, and likewise increases in H/C at constant O/C are hydrogenation paths (**A** in Figure 8.1). Since (H/C)/(O/C) = H/O, the H/O ratio is given by the slope of any trajectory at the appropriate point. Straight lines at 45° to the O/C axis (**D** in Figure 8.1) correspond to dehydration since they represent loss of one oxygen atom for every two hydrogen atoms disappearing (in van Krevelen' plot, the O/C scale is spaced out to twice the H/C scale to confer this property). Chemical reactions involving carbon must be represented in quite a different way. For example, since carbon dioxide has an atomic O/C ratio of 2 and an atomic H/C ratio of zero, decarboxylation would cause any composition to move away from the point O/C = 2, H/C = 0. Thus decarboxylation would be represented by lines radiating out from this point in all directions (**E** in Figure 8.1); this was proved algebraically by van Krevelen. Similarly demethanation would be represented by lines radiating out in all directions from the point H/C = 4, O/C = 0 (**C** in Figure 8.1).

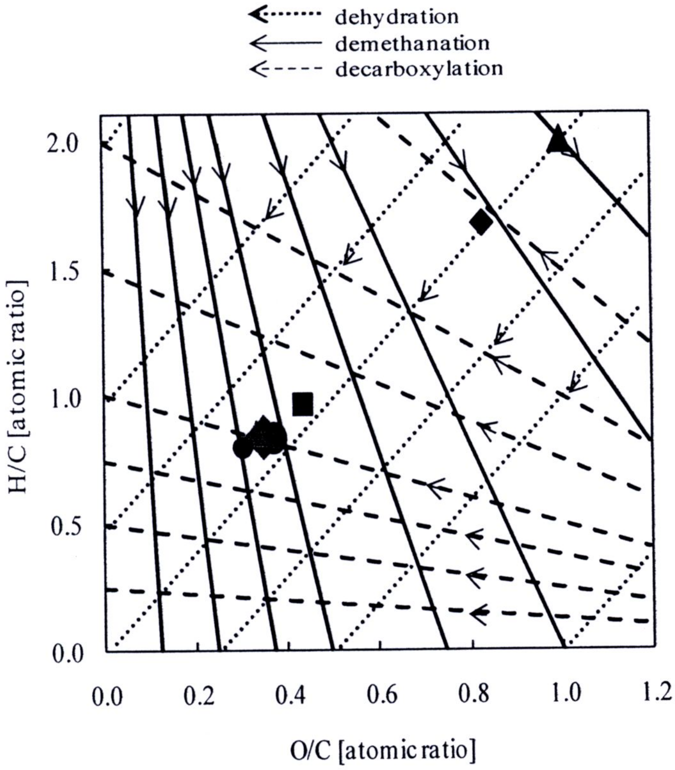

Figure 8.2 H/C versus O/C van Krevelen diagram of the synthesized CMSs from hydrothermal process with initial concentration of 10wt%, 180°C, 24h; (▲ = glucose), (◆ = native corn starch), (■ = CMSs from glucose), (● = CMSs from amylopectin), (■ = CMSs from amylopectin+amylose), (◆ = CMSs from HI-CAP®100,), (▲ = CMSs from amylose), and (● = CMSs from native corn starch)

These changes were analyzed by means of a van Krevelen diagram (see Figure 8.2). This graph offers the advantage that the elemental reactions that occur during carbonization can be represented by straight lines that describe the dehydration, decarboxylation, and demethanation processes. The evolution from the carbohydrates to the CMS samples follows the diagonal line, which suggests that dehydration reactions prevail during hydrothermal carbonization. In this process possibly ether, anhydride, and lactone bonds are formed. It should also be noted that the location of the CMS samples in the H/C versus O/C diagram is far away from that of the coal, which has a lower O/C ratio as a consequence of decarboxylation and demethanation reactions that take place during natural coalification [72].

The percentage of carbon fixed in the CMS particles can be calculated from the comparison of the chemical composition of the starting carbohydrate and that of the final carbon material (shown in Table 8.1). Thus, depending on the operational conditions (i.e., temperature, reaction time, and type of carbohydrate), about 80% of the carbon contained in the carbohydrate is retained in the CMSs (as shown in Table 7.1, Chapter 7). The parameter that influences to a higher extent the carbon fixation in the CMSs is the reaction temperature, as it is the parameter with a major influence on the product yield (see Table 7.1, in Chapter 7).

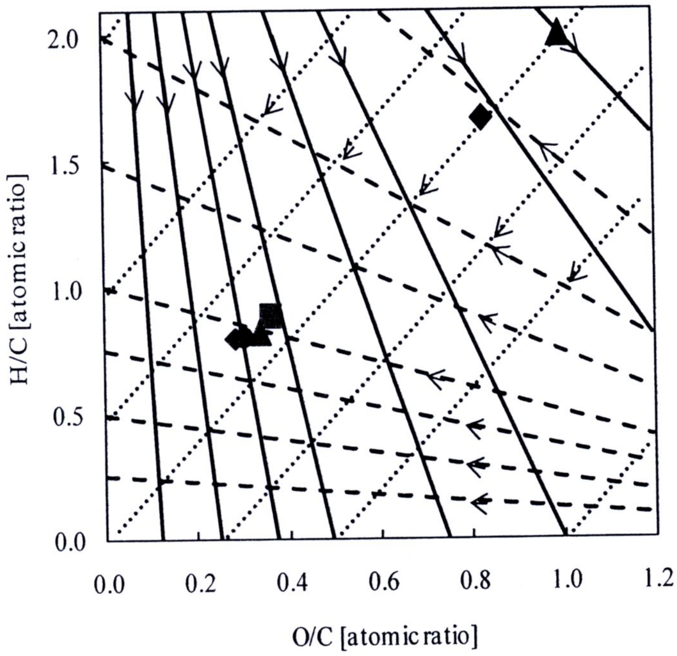

Figure 8.3 H/C versus O/C van Krevelen diagram of the carbon microspheres; (▲=glucose), (◆=native corn starch), (■=CMSs from native corn starch 10wt%, 180°C, 6h), (▲=CMSs from native corn starch 10wt%, 180°C, 18 h), (●=CMSs from native corn starch 10wt%, 180°C, 24h) and (◆=CMSs from native corn starch 10wt%, 220°C, 6h)

8.3.2 Chemical structure analysis by FT-IR technique

The changes in the chemical characteristics of the carbohydrates that take place during the hydrothermal process have been investigated by FT-IR spectroscopy techniques. The FT-IR spectra corresponding to the CMS samples were shown in Figure 8.4.

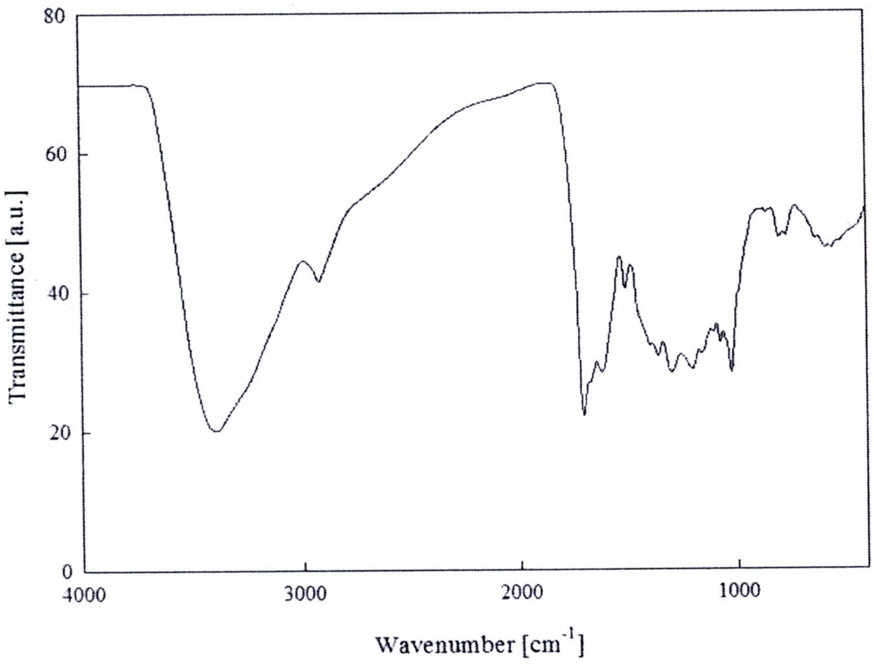

Figure 8.4 FTIR spectra of the CMS samples obtained by hydrothermal process of native corn starch with initial concentration of 10wt% at 180°C for 24h

The bands at 1710 and 1620 cm^{-1} (together with the band at 1513 cm^{-1}) can be attributed to C=O (carbonyl, quinone, ester, or carboxyl) and C=C vibrations respectively, whereas the bands in the 1000–1450 cm^{-1} region correspond to C-O (hydroxyl, ester, or ether) stretching and O-H bending vibrations [12]. The bands at 875–750 cm^{-1} are assigned to aromatic C-H out-of-plane bending vibrations, whereas the bands at approximately 2900 and 3000–3700 cm^{-1} correspond to stretching vibrations of aliphatic C-H and O-H (hydroxyl or carboxyl), respectively [32]. A comparative analysis of the FTIR spectra of the carbon microspheres (Figure 8.4) suggests that dehydration and aromatization processes take place during the hydrothermal carbonization, which confirms the results deduced from the van Krevelen diagram in the previous section. Thus, the intensities of the bands corresponding to the hydroxyl or carboxyl groups (3000–3700 and 1000–1450 cm^{-1}) in the carbon microspheres are weaker than those of the corresponding carbohydrates, thereby disclosing dehydration reactions [73]. New vibration bands at 1710 cm^{-1}, corresponding to C=O groups, and 1620 and 1513 cm^{-1}, corresponding to C=C groups, appear in the carbon microspheres material [74]. The appearance of the bands at 1620 and 1513 cm^{-1} reveals the aromatization of the samples [30]. An increase in the temperature of the hydrothermal process of glucose is accompanied by a diminution in the intensities of the band at 1710 cm^{-1} (C=O) and the wide band at approximately 3000–3700 cm^{-1} (O-H), due to oxygen removal [15]. At the same time, both the aromatic hydrogen and aromatic carbon (C=C) content increase, as evidenced by the increase in the intensity of the bands at 875–750 cm^{-1} and 1620 cm^{-1}, respectively [75]. These data reveal an increase in the aromatization of the carbon microspheres as the reaction temperature rises, which is the normal tendency for a carbonization process.

8.3.3 Carbon microsphere formation mechanisms from glucose

As the temperature was raised, the CMS formation was observed and accelerated. From these experimental observations, the glucose, hence, proceeded through three different reaction pathways concurrently in hydrothermal process, that is, decomposition, isomerization and dehydration [31]. In the first pathway, glucose decomposed into a liquid product (TOC) consisting of acid and aromatic compounds, e.g., levulinic acid, 1,2,4-benzenetriol, 1,4-benzenediol, 5-methyl-2-furaldehyde, and furfural [32]. The reactions included furan ring hydrolysis and pyrolysis. The decomposition pathway of glucose was independent from its initial concentration. The last pathway—the dehydration, produced many reactive intermediates such as 5-HMF, furfural which is assumed are mainly substances for CMS formation [33]. The FT-IR analysis of CMS particles illustrated the presence of the 5-HMF functional groups in the char structure, implying the possible polymerization among the 5-HMF molecules to form CMSs. The polymerization was possibly via substituent functional groups and ring substitution in order to preserve the 5-HMF structure in the CMS particles [66]. Further carbonization was also possible. From these observations and assumptions, we propose an overall CMS formation pathway from glucose in hydrothermal process (see Figure. 8.5).

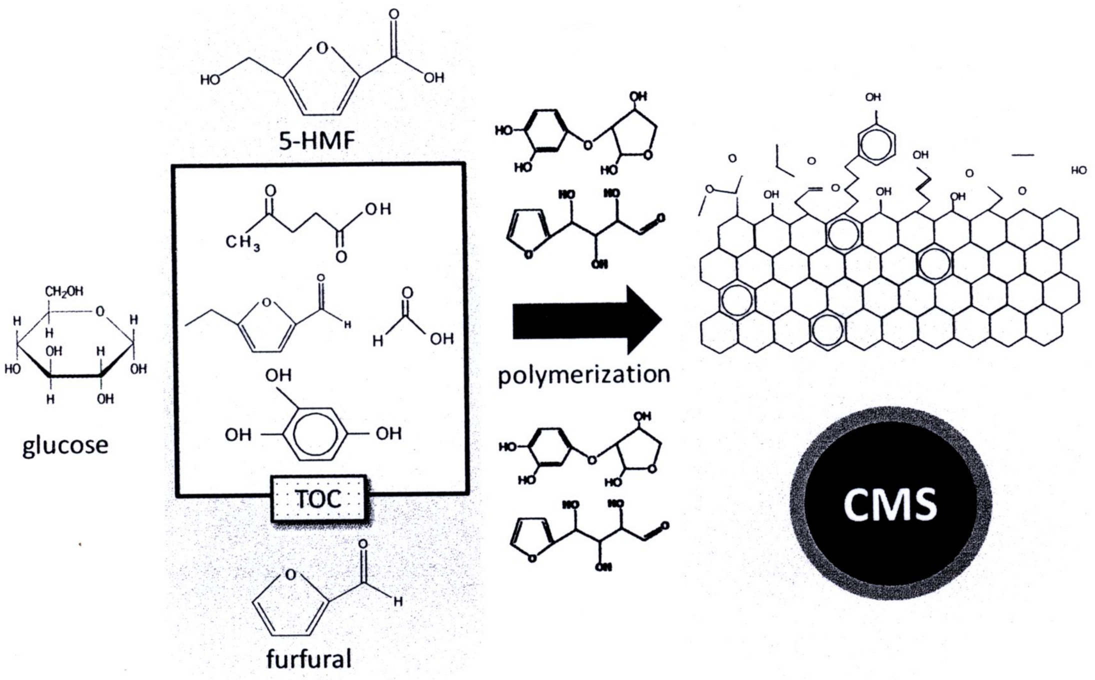

Figure 8.5 Proposed CMS formation pathway from hydrothermal process of glucose

8.3.4 Kinetic model for hydrothermal process of glucose

8.3.4.1 Liquid product and intermediates determination

According to Chuntanapum et al., three main pathways for glucose reaction are possible under the subcritical condition; the reaction predominantly yield 5-HMF via the dehydration of the glucose, the reaction yield TOC compounds via the decomposition of glucose, the reaction yield fructose via the isomerization of glucose [32]. Although many reactions are occurred in hydrothermal of glucose, some intermediates are though that mainly contribution for carbon microsphere formation such as 5-HMF, furfural, and TOCs. 5-HMF was main intermediate to form char or tarry materials [31]. Moreover, furfural is one of furan compounds which are also polymerized reactively to form solid product. However, many compounds in decomposition of glucose cannot be identified which are defined as TOC compounds (lumped total organic carbon). According to three main compounds for carbon microspheres formation, we decided to indentify these intermediates for proposing CMS formation mechanisms. The reaction pathway was proposed to find kinetic parameters as shown in Figure 8.6.

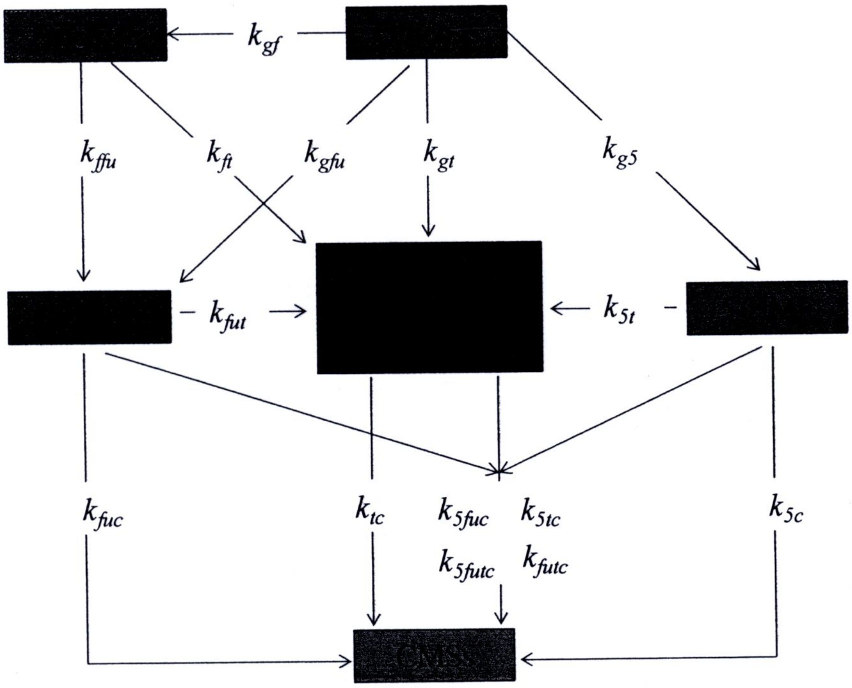

Figure 8.6 Reaction pathway of carbon microspheres formation from hydrothermal process of glucose [31]

Given that TOCs are key compounds in the subcritical (as intermediates in the carbon microsphere production pathway). We decided to identify the TOC compounds by TOC analyzer. As it turned out, however, neither levulinic acid nor formic acid was detected. pH measurements revealed that the liquid effluents were more acidic than the initial glucose solution (pH 6.6). The pH values of the liquid effluent in the experiments conducted at 140, 180 and 220°C, for example, were in the ranges of 5.5 – 5.0 and 4.7 – 5.5, and 3.5 – 4.5 respectively. This suggested that a range of acid molecules are formed in the aqueous phase. The actual compounds formed, however, could not be specified. Unexpectedly, fructose, 5-HMF, furfural are relatively small observed in all experiments which may be caused from these intermediates were nearly consumed to produce solid product.

8.3.4.2 Glucose decomposition behavior

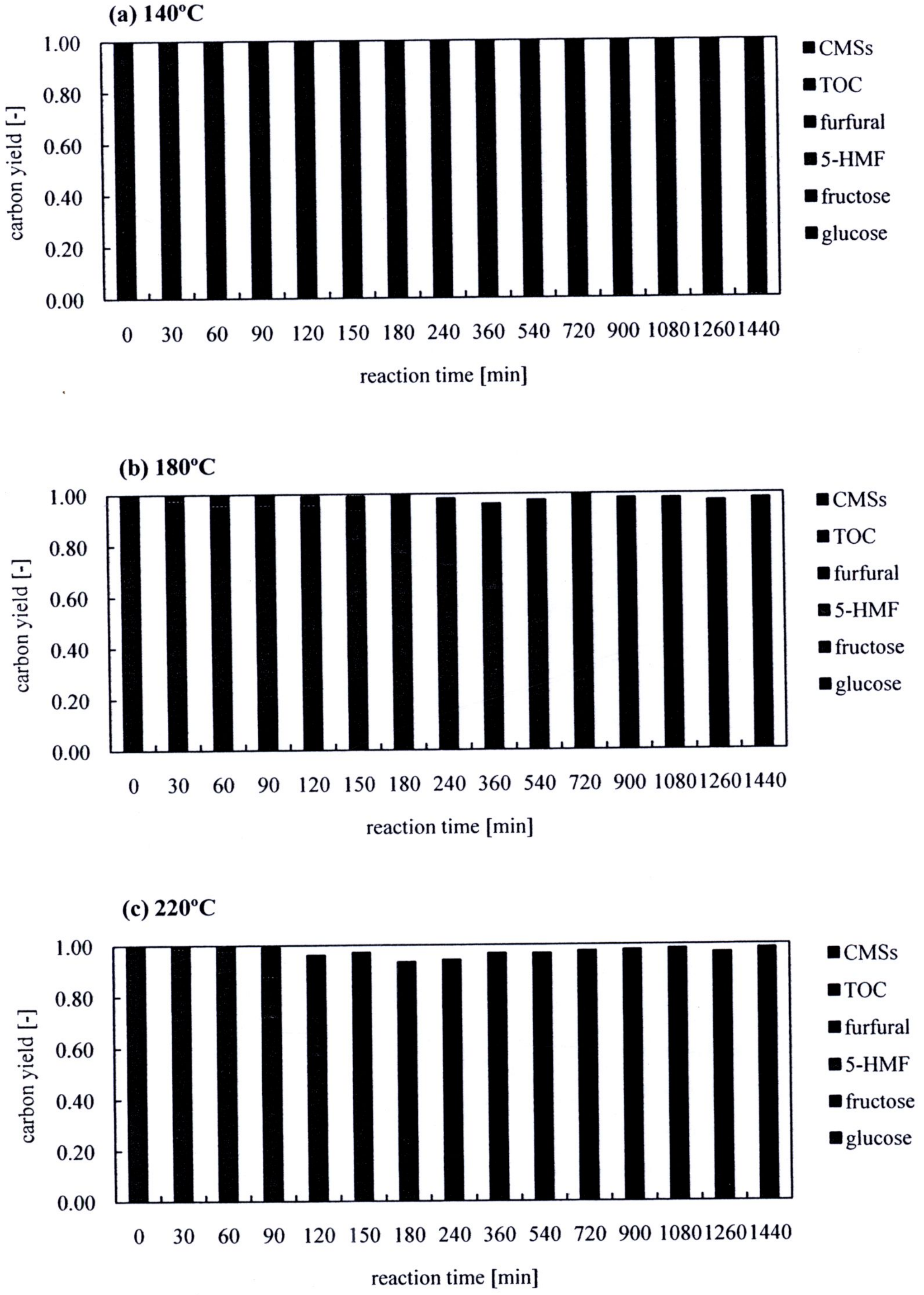

Figure 8.7 Carbon balance: carbon content in liquid products and solid products compared to that in initial glucose of 10wt%, for the experiments conducted at 140, 180 and 220°C

(a)

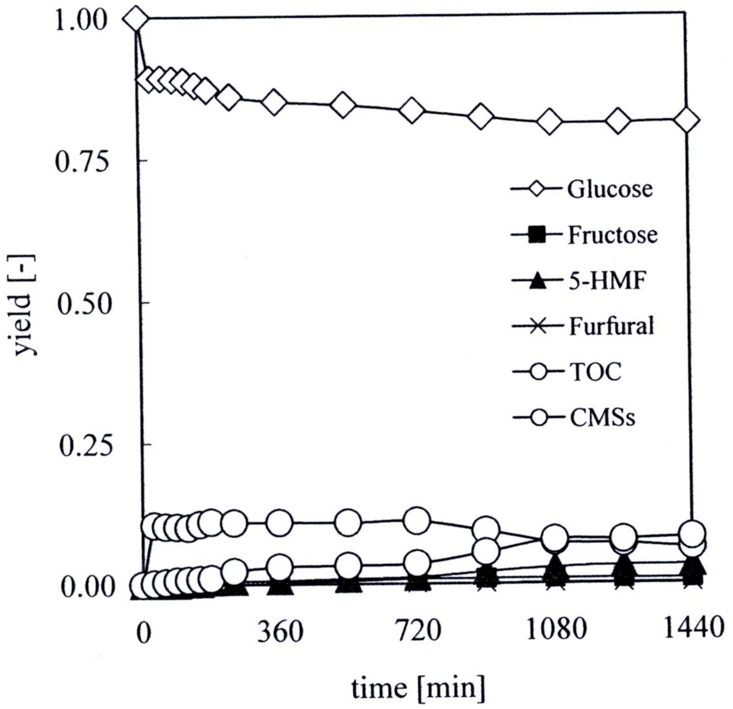
1.00
0.75
0.50
0.25
0.00
yield [-]
0
360
720
1080
1440
time [min]
Glucose
Fructose
5-HMF
Furfural
TOC
CMSs

(b)

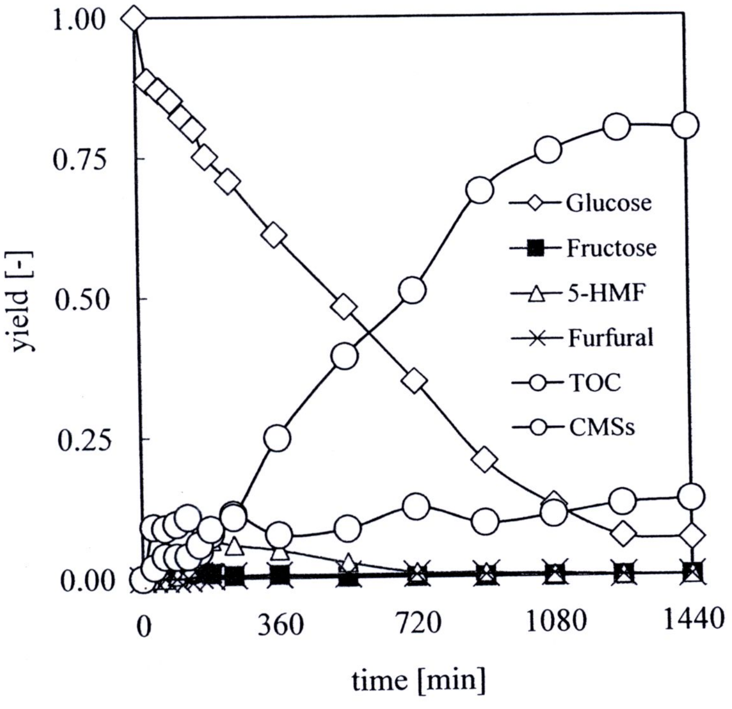
1.00
0.75
0.50
0.25
0.00
yield [-]
0
360
720
1080
1440
time [min]
Glucose
Fructose
5-HMF
Furfural
TOC
CMSs

(c)

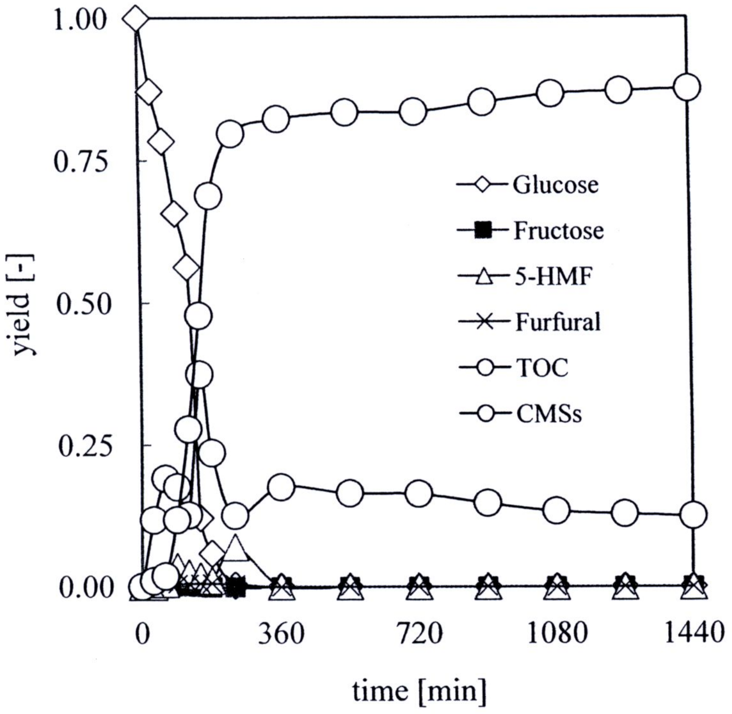

Figure 8.8 Relative product yields for hydrothermal process of glucose with initial concentration of 10wt% at reaction temperature of (a) 140, (b) 180°C and (c) 220°C, and reaction time from 0 to 1440 min

From Figure 8.8(b), we can observe a small lag time between the beginning of glucose decomposition and the appearance of the solid product. In other words, glucose yield decreased rapidly at the beginning of the reaction but an increase of solid product took time to respond this rapid change. This time difference, the so-called "induction time", is characteristic of serial reactions. Moreover, a decrease in the TOC yield at high temperature and long reaction time (i.e., 220°C and from 150 min) is also the sign of its being intermediate of the serial reactions. By these observations, we assume that glucose initially decomposes into the liquid product, whereupon the liquid product acts as an intermediate compound to form the solid product. The decomposition behavior is assumed to follow the first-order serial reaction is shown in Figure. 8.6.

8.3.4.4 Assumptions for kinetic modelling

To find kinetic model for describing the reaction that occur during hydrothermal carbonization of starch was difficult to determine every intermediates because the reaction consist of many reaction (multiple reaction, series reaction, parallel reaction, and reversible reaction). However, the assumption was generally used to provide a kinetic study in this reaction more simply. In hydrothermal carbonization of glucose, glucose can isomerize to yield fructose, namely reversible reaction. To simplify this complicated reaction, we assumed that all reaction that occurs during hydrothermal carbonization of glucose is non-reversible reaction. Moreover, all reaction which was proposed in the reaction is elementary reaction. Finally, pseudo-first order reaction was employed to fit the experimental data. In the specific experimental condition and all stated assumptions, it was found that the experimental data was obeyed with the model. The assumptions were used in this kinetic study as follows:

1.) All occurred reaction was non reversible reaction,

2.) All reaction was elementary reaction,

3.) Pseudo first order kinetic was assumed.

From the proposed reaction pathway, rate equations can be derived in order to calculate rate constants. The rate equations, hence, can be written as follows [31]:

$$\frac{d[glucose]}{dt} = -(k_{gf} + k_{gfu} + k_{gt} + k_{g5})[glucose], \tag{8.1}$$

$$\frac{d[fructose]}{dt} = k_{gf}[glucose] - (k_{f5} + k_{ffu} + k_{ft})[fructose], \tag{8.2}$$

$$\begin{aligned} \frac{d[5-HMF]}{dt} = {} & k_{g5}[glucose] + k_{f5}[fructose] - k_{5t}[5-HMF] \\ & - k_{5c}[5-HMF] - k_{5futc}[5-HMF][furfural][TOC] \\ & - k_{5fuc}[5-HMF][furfural] - k_{5tc}[5-HMF][TOC], \end{aligned} \tag{8.3}$$

$$\begin{aligned} \frac{d[furfural]}{dt} = {} & k_{gfu}[glucose] + k_{ffu}[fructose] - (k_{fut} + k_{fuc})[furfural] \\ & - k_{5futc}[5\text{-}HMF][furfural][TOC] - k_{5fuc}[5-HMF][furfural] \\ & - k_{futc}[furfural][TOC], \end{aligned} \tag{8.4}$$

$$\begin{aligned} \frac{d[TOC]}{dt} = {} & k_{gt}[glucose] + k_{ft}[fructose] + k_{5t}[5-HMF] + k_{fut}[furfural] \\ & - k_{tc}[TOC] - k_{tg}[TOC] - k_{5futc}[5-HMF][furfural][TOC] \\ & - k_{5tc}[5-HMF][TOC] - k_{futc}[furfural][TOC], \end{aligned} \tag{8.5}$$

$$\begin{aligned} \frac{d[CMSs]}{dt} = {} & k_{fuc}[furfural] + k_{5c}[5-HMF] + k_{tc}[TOC] \\ & + 3k_{5futc}[5-HMF][furfural][TOC] + 2k_{5fuc}[5-HMF][furfural] \\ & + 2k_{5tc}[5-HMF][TOC] + 2k_{futc}[furfural][TOC], \end{aligned} \tag{8.6}$$

where, [*glucose*] = glucose concentration (mol-C/L),

[*fructose*] = fructose concentration (mol-C/L),

[*5-HMF*] = 5-HMF concentration (mol-C/L),

[*furfural*] = furfural concentration (mol-C/L),

[*TOC*] = lumped carbon concentration of the other liquid products (mol-C/L),

[*CMSs*] = carbon microspheres concentration (mol-C/L),

k_{ij} = rate constant (min^{-1}),

t = reaction time (min).

8.3.4.5 Iteration procedure

The iteration was carried out to find all the kinetic parameters (the rate constants k_{ij} and the orders of the reaction α_{ij}) in the equations 8.1-8.6 that gave the best fitting between the calculated and experimental values. The criterion of the numerical calculation was the least square of error (LSE) [31]:

$$LSE = \min_{x}\left(\sum([\exp]-[cal]_x)^2\right), \tag{8.7}$$

where, [exp] = the experimental concentration (mol-C/L),

$[\mathrm{cal}]_{\mathrm{x}}$ = the calculated concentration predicted by the set of kinetic parameters x (mol-C/L).

The iteration stops when the set of kinetic parameters x that satisfy the equation 8.7 is found. The experimental results obtained from the experiments of glucose of 10 wt% were used for the fitting. The non-linear regression with least square of error (i.e., the difference between the experimental and calculated values) as a criterion was applied to fit the model with the experimental data. Figure 8.9 plots the calculated values in solid line and experimental values in bullets. When all the reactions are assumed to be first-order, the fit between the model and experiment is reasonable as shown in Figure 8.9. The comparison between the experimental and the calculated glucose yields is also shown separately in Figure 8.10. The rate constants obtained are shown in Table 8.2. Although the fitting seems reasonable in general, the limitations of the first-order model have been stated in many publications.

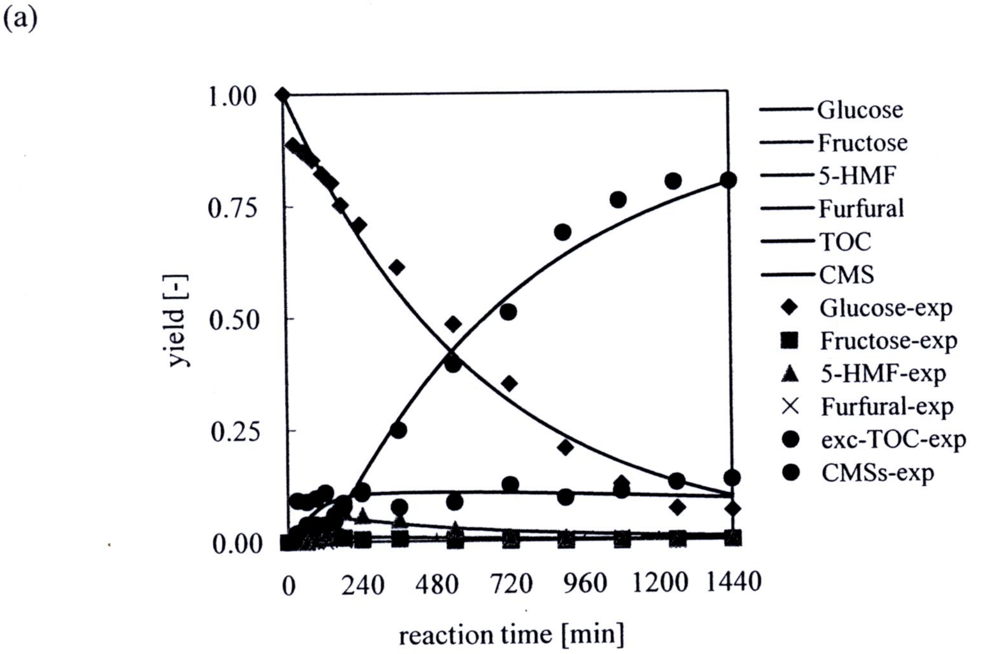

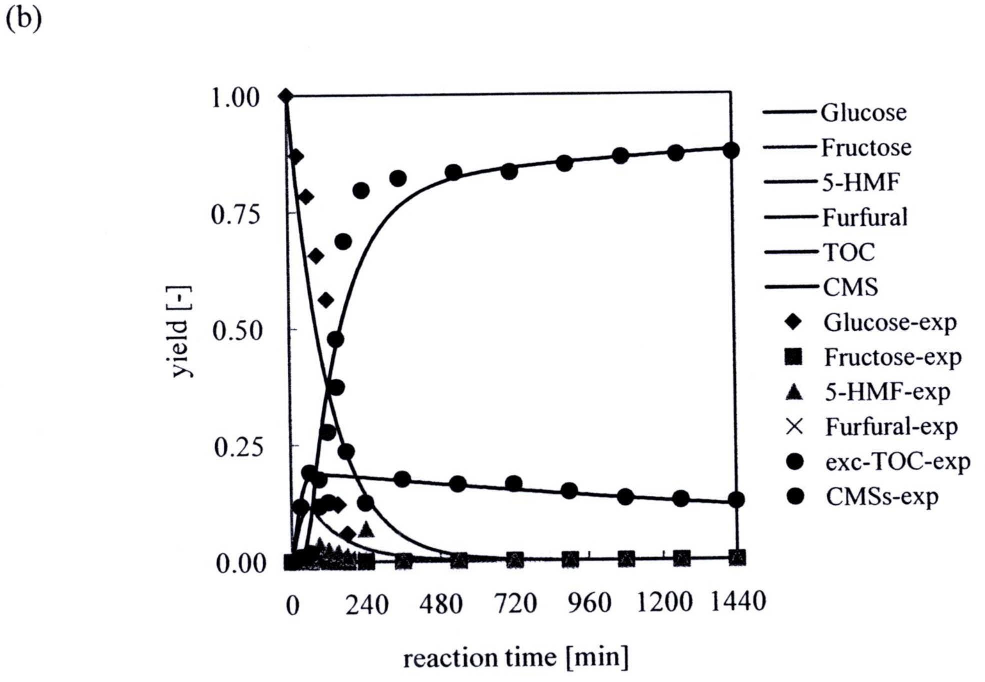

Figure 8.9 Product yields based on carbon content, at temperatures of (a) 180°C and (b) 220°C, and reaction times from 0 to 1440 min (symbols [experimental data]; lines [model predictions])

In generally, the mechanism of solid product formation is more complicated: it might involve many transition steps and compounds, and the proposed model cannot completely explain it. Nonetheless, the model seems to effectively demonstrate, albeit in a general fashion, that solid product is produced through the formation of liquid product rather than directly from glucose. The concentration of the liquid product rises in parallel with the reaction time, and the solid product gradually increases afterwards. A continuous increase in the solid product with both reaction time and temperature finally leads to a decrease in the concentration of the liquid product, as can be observed from the experiment conducted at 220°C, and at the reaction time of 150 min onwards.

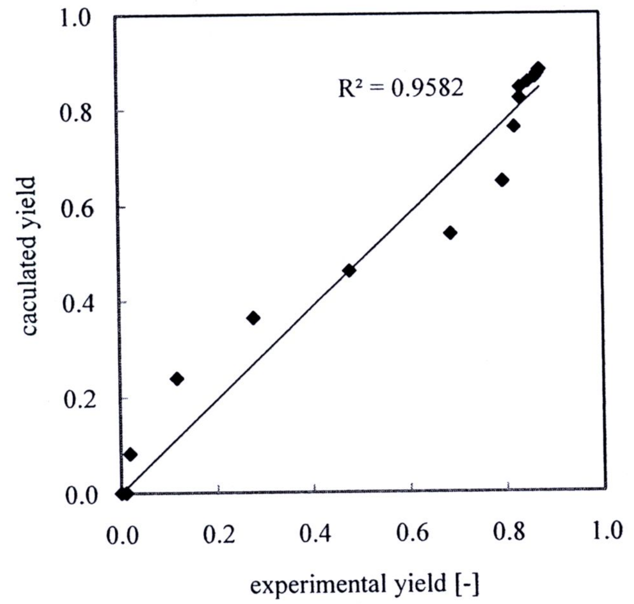

Figure 8.10 Parity plot between experimental and calculated values of CMSs yield

Figure 8.10 also shows the calculated values (represented by solid lines) for comparison with the experimental data. The model predictions seem to fit the experimental data fairly well, both in the graphs and as suggested by the high r^2 (determination coefficient) value obtained from the parity plots between the experimental data against the calculated data. Among the three results, the model is in better agreement with the glucose decomposition behavior. This implies that the exponentially decayed decomposition behavior of glucose can be explained well by the first-order reaction.

Table 8.2 Reactions and kinetic parameters of carbon microsphere formation in hydrothermal process of glucose with initial concentration of 10wt% at 180°C

Kinetic parameters	Type of reaction	k_{ij} (mol-C/L)min^{-1}	α (-)
k_{gf}	isomerization	$1.42\text{x}10^{-4}$	1
k_{gfu}	dehydration	$3.42\text{x}10^{-5}$	1
k_{gt}	decomposition (many reaction)	$8.76\text{x}10^{-4}$	1
k_{g5}	dehydration	$5.30\text{x}10^{-4}$	1
k_{f5}	dehydration	0	1
k_{ffu}	dehydration	$8.76\text{x}10^{-3}$	1
k_{ft}	decomposition (many reaction)	0	-
k_{5t}	decomposition (many reaction)	0	-
k_{5c}	polymerization	$1.00\text{x}10^{-7}$	1
k_{fut}	decomposition (many reaction)	$2.09\text{x}10^{-3}$	1
k_{fuc}	polymerization	0	-
k_{tc}	polymerization	$3.79\text{x}10^{-4}$	1
k_{5futc}	polymerization	$1.00\text{x}10^{-6}$	1
k_{5tc}	polymerization	$2.23\text{x}10^{-2}$	1
k_{5fuc}	polymerization	$1.00\text{x}10^{-7}$	1
k_{futc}	polymerization	0	-

As the reaction rate constants listed in the Table 5.5, the main decomposition of glucose was inferred from the higher rate constants which are k_{gf}, k_{gt}, k_{g5}. From the previous experiment showed that 5-HMF was resisted to decompose in low temperature [32]. This result was observed in this experiment. Therefore, 5-HMF tends to polymerize to from carbon product. The main pathway was thought to show strong effect on carbon solid product which was polymerization of 5-HMF and TOC compound.

Table 8.3 Reactions and kinetic parameters of carbon microsphere formation in hydrothermal process of glucose with initial concentration of 10wt% at 220°C

Kinetic parameters	Type of reaction	k_{ij} (mol-C/L)min^{-1}	α (-)
k_{gf}	isomerization	0	-
k_{gfu}	dehydration	0	-
k_{gt}	decomposition (many reaction)	4.30×10^{-4}	1
k_{g5}	dehydration	2.91×10^{-3}	1
k_{f5}	dehydration	9.62×10^{-6}	1
k_{ffu}	dehydration	1.456×10^{-4}	1
k_{ft}	decomposition (many reaction)	4.26×10^{-4}	1
k_{5t}	decomposition (many reaction)	0	-
k_{5c}	polymerization	1.00×10^{-14}	1
k_{fut}	decomposition (many reaction)	7.04×10^{-4}	1
k_{fuc}	polymerization	2.83×10^{-8}	1
k_{tc}	polymerization	3.44×10^{-4}	1
k_{5futc}	polymerization	9.54×10^{-6}	1
k_{5tc}	polymerization	3.21×10^{-2}	1
k_{5fuc}	polymerization	4.23×10^{-6}	1
k_{futc}	polymerization	0	-

From the reaction rate constants listed in the table 8.3, it was found that isomerization and dehydration of glucose to yield fructose and furfural respectively was observed in the reaction temperature of 180°C. This result was caused from the higher temperature (220°C) which affects on other reaction play an important role. At 220°C, dehydration of glucose to yield 5-HMF had a higher rate constant than the rate constant at 180°C.

8.3.5 Modified reaction pathway for hydrothermal process of native corn starch

For using native corn starch as carbon precursor for CMS formation, the reaction pathway of glucose could be modified to propose reaction pathway of CMS formation from native corn starch as shown in Figure 8.11. In this pathway, native corn starch can be hydrolyzed to yield both of glucose and TOC compounds. Reaction rate constants (k_{sg} and k_{st}) were introduced to describe hydrolysis reaction of native corn starch.

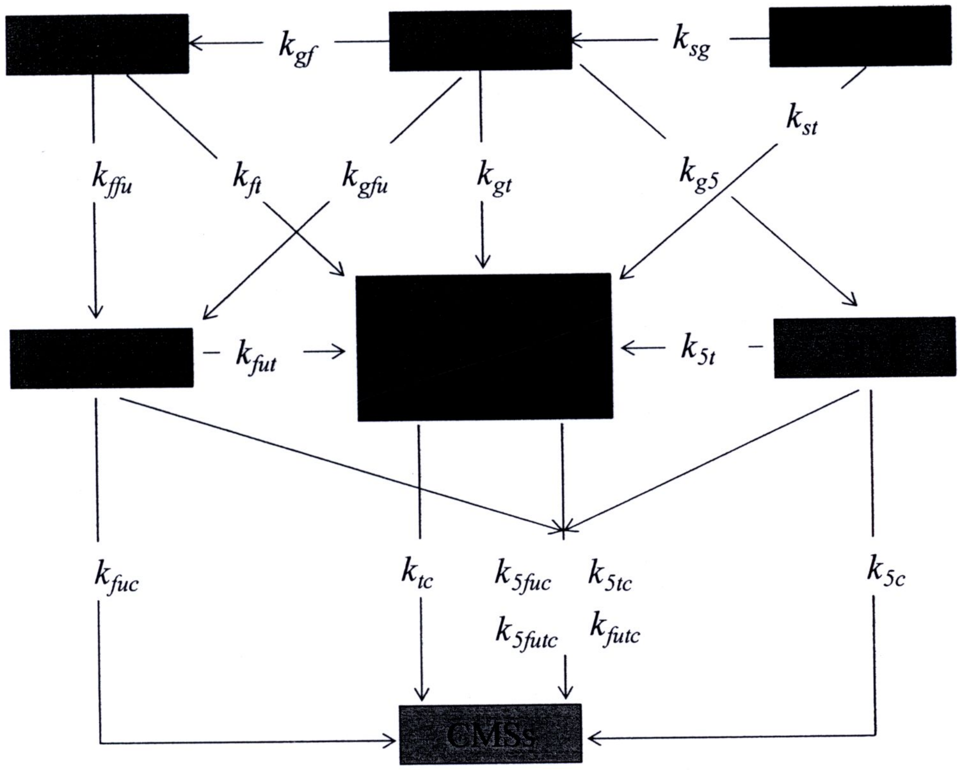

Figure 8.11 Reaction pathway of carbon microsphere formation from hydrothermal process of native corn starch [31]

From this reaction pathway, we can address the rate equations and fit reaction model to obtain rate constants. However, pseudo-first order reaction cannot fit many reactions during hydrothermal process because the native corn starch has structure which was difficult to be hydrolyzed. The fitting results were provided in an appendix B for preliminary step in further study.

8.4 Conclusions

The as-prepared CMS particles had a different chemical structure due to types of carbon precursor. The CMSs from hydrothermal of glucose had less an O/C and H/C ratio than the CMSs from hydrothermal of starch because glucose had an O/C and H/C ratio than starch. The increase both of reaction time and reaction temperature also strongly affected on increasing of an O/C and H/C ratio. From van Krevelen prediction and FT-IR results, we can address an overall reaction which was a dehydration reaction. Moreover, first order reaction assumption can be fitted well with the experimental data from glucose experiment and the rate constants were obtained. CMS formation reaction from glucose could be described by reaction pathway through many intermediates (mainly TOC, 5-HMF and furfural). Nevertheless, first order reaction model cannot fit the experimental data from hydrothermal process of native corn starch because native corn starch was difficult to be hydrolyzed to obtain glucose. In addition, from FT-IR and TEM results, the synthesized CMSs consisted of dense aromatic carbon ring as a core and reactive hydrophilic group as a shell.